



# Internal Heterogeneity in a Reactive Powder Concrete

O Bayard, O Ple, G Bernier

## ► To cite this version:

O Bayard, O Ple, G Bernier. Internal Heterogeneity in a Reactive Powder Concrete. 6th RILEM Symposium on Fibre-Reinforced Concretes, Sep 2004, Varenna-Lecco, Italy. pp.20 - 22. hal-01099841

**HAL Id: hal-01099841**

**<https://hal.science/hal-01099841>**

Submitted on 5 Jan 2015

**HAL** is a multi-disciplinary open access archive for the deposit and dissemination of scientific research documents, whether they are published or not. The documents may come from teaching and research institutions in France or abroad, or from public or private research centers.

L'archive ouverte pluridisciplinaire **HAL**, est destinée au dépôt et à la diffusion de documents scientifiques de niveau recherche, publiés ou non, émanant des établissements d'enseignement et de recherche français ou étrangers, des laboratoires publics ou privés.

## Internal Heterogeneity in a Reactive Powder Concrete

O. BAYARD<sup>1)</sup>, O. PLE<sup>2)</sup>, G. BERNIER<sup>3)</sup>

<sup>1)</sup> Head of the Ductal<sup>®</sup> Division, Lafarge Ciments, 5 bd L. Loucheur, 92214 Saint-Cloud, France

<sup>2)</sup> LIRIGM, Université Joseph Fourier, BP 53, 38041 Grenoble Cedex 9, France

<sup>3)</sup> LMT, E.N.S de Cachan, 61 Avenue du Président Wilson, 94235 Cachan Cedex, France

### Abstract

Reactive Powder Concrete (RPC) is made of a very fine homogeneous and compact matrix with short steel fibres. Internal heterogeneities in the material induce heterogeneities of the mechanical characteristics. Elastic fields are disturbed by the presence of fibres. These fields within the matrix, such as load transfers, which operate between fibres and the surrounding matrix, depend not only on the mechanical characteristics of each component, but also on the local percentage of fibres and the local orientation of fibrous reinforcement.

During preparation of RPC, the fibrous suspension is concentrated in solution. The result is a unique distribution of fibres by clusters within the structure.

In this paper, we propose a study of the mechanical behaviour of RPC elements by use of a numerical approach that takes internal heterogeneities into account. Specific structural elements are tested under both tension and flexion. A comparison between the numerical approach and our experimental investigations confirms the influence of internal heterogeneities on mechanical behaviour. This study therefore is aimed at providing some indications of the role played by heterogeneities induced by the casting process and their potential use in optimising the mechanical behaviour of fibre-reinforced RPC.

### 1. Introduction

Reactive Powder Concrete (RPC), also called Ductal<sup>®</sup>, is a new generation of concrete and features ultra-high performance. This specific material is composed of very fine sand powders (diameters less than 500 microns), cement, fillers, silica fume, a small water-to-cement ratio ( $W/C = 0.22$ ), and recently-developed superplasticizers [1]. The improvement in ductility of such a ceramic may be obtained by adding short metallic fibres (length: 13 mm, diameter:  $d_f = 0.16$  mm) [2]. This type of concrete is often used in slender structures with no passive reinforcement, such as the Seonyu Footbridge [Fig. 1].



**Fig. 1:** Seonyu Footbridge built with RPC



**Fig. 2:** Size of fibre cluster

The percentage of metallic fibres used in this material is quite high (over 2% on a volume basis) and leads to a specific distribution of fibres within the structure [3]. The consequence then is to produce a local alignment of fibres, under the effect of strong shear gradients, coupled with wall effects and a regrouping of fibres by clusters due to the casting process. The size of the clusters observed during experiments is approximately 20-40 mm, depending on the mode of casting [Fig. 2].

Within the structure, we must accommodate both an initial study scale relative to the aligned fibre cluster and a second scale relative to the interaction between the clusters themselves [Fig. 3, page 10/10]. Since the typical field of application of RPC pertains to small-sized, highly-streamlined structural elements, the dimensions of the structure are close to the size of fibre clusters. The mechanical behaviour of a structure is thus coupled with the mechanical behaviour of interacting clusters. To diagram such a specific distribution of reinforcement within various structures, a modelling approach by cells, which includes a parallel fibre cluster [4-6], will be presented herein. The orientation and density of fibres in each cluster constitute parameters that are governed by both the mode of casting and the structural strength, as well as by the way the damage process is influenced [4] [Fig. 4].

In order to model the mechanical performance of such a structure, we first need to diagram the distribution of fibres and interactions between clusters within the structure; this is the topic of the present paper.

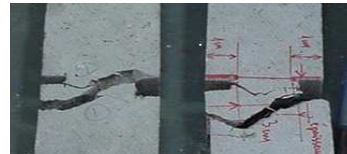


**Fig. 4:** Deviation and orientation of cracking by fibres

## 2. Modelling elastic mechanical behaviour

The schematic presentation at various scales induces the modelling of stress and strain fields at three different scales: local scale (fibre), the meso-local scale (cluster and cell), and the global scale (structure). The stress and strain distributions in a cell at the local and meso-local scales are identified by Eshelby's analytical laws [7,8]. Figure 5 presents the evolving nucleation criterion, as induced by strain localisation in an isolated cell with a spherical cluster of 2% per volume of fibres, with the inclination ( $\alpha$ ) of fibres related to an applied uniaxial tensile strain [Fig. 5]. This criterion is based on the notion of equivalent strain, in order to evaluate the tensile strain in 3D space.

$$\tilde{\varepsilon} = \sqrt{\langle \varepsilon_1 \rangle_+^2 + \langle \varepsilon_2 \rangle_+^2 + \langle \varepsilon_3 \rangle_+^2} \quad (1)$$

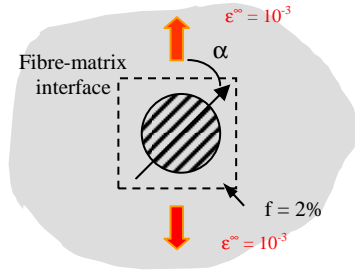
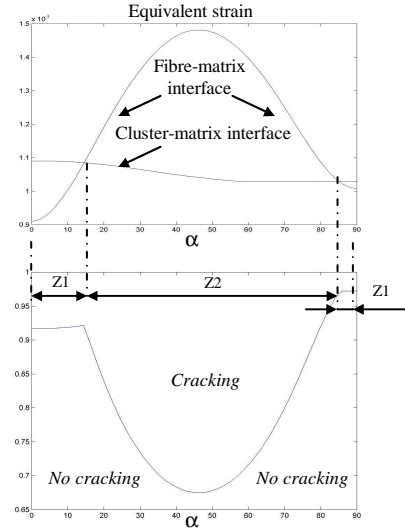


**Fig. 5:** Crack nucleation criterion within an isolated cell submitted to tensile strain  
Z1: Cracking at the cluster-matrix interface  
Z2: Cracking at the fibre-matrix interface (inside the cluster)



These stress and strain distributions are then converted into an average stress and strain induced within the cell by this cell's environment in the structure. These global fields are determined by use of the finite element method. Each Q8 of this model corresponds to a cell (one density, one fibre direction, one cluster shape). The equivalent homogeneous stiffness of this Q8 is a numerical average of the stiffness at each point of the cell, as explained by Eshelby's inclusion theory [7,8].

$$R_{cellule(i)}^{eq} = \frac{1}{N_{pts}} \sum_{n=1}^{N_{pts}} \left[ R_n^{cellule(i)} + \sum_{m=1}^{M_{voisins}^{cellules} = 26} R_{cellule(m)}^{pts(n)} \right] \quad (2)$$

In this manner, the localisation of strains and stresses at the fibre-matrix interface on the local scale and the effect at the global scale can then be derived. Similarly, stress and strain localisation at the cluster-matrix interface can also be modelled (the meso-local scale). Thanks to the finite element method and an arbitrary global distribution of both fibre density and orientation within the cells composing any structure, we are able to determine, under an arbitrary loading, the stress and strain distribution at each point in this structure. Nucleation of the initial crack as well as the damage process have also been studied.

When cracking appears on a very small scale under tensile strain, fibres intervene in order to prevent the microscopic crack from being propagated and from causing ruin of the structure [6]. During multi-cracking of the material, an action known as "crack bridging" by fibres involves many micro-mechanisms, whose level of loading depends on the angle existing between the direction of local reinforcement (fibres) and the normal to the cracking plane. In addition to these micro-mechanisms, other phenomena may appear, such as: bond and slip at the fibre-matrix interface [9-12], friction [13,14] and remote pinching [15], as well as local moments related to local fibre-bending [16].

Modelling the action of these fibres relative to the local crack orientation and all corresponding micro-mechanisms is made possible through the use of phenomenological laws of the 3D damage process. These laws have been extracted from the mechanical behaviour of specific structures produced with an arbitrarily-inclined fibre orientation with respect to a single tensile direction. The 1D damage laws, which correspond to various fibre inclinations relative to the primary tensile direction, are assembled according to micro-plane theory in order to determine, using an equivalent energy-based method, the 3D damage laws.

### 3. Mechanical behaviour under tension

Specific specimens, reinforced by means of oriented fibres, have been tested under uniaxial tensile stress [Fig.6]. Tests were conducted on 120 samples. To obtain the test samples, specific cuts were operated on a concrete block with oriented fibres and then assigned an orientation  $\alpha$  equal to  $0^\circ$ ,  $30^\circ$ ,  $45^\circ$ ,  $60^\circ$  and  $90^\circ$  [Fig. 6].

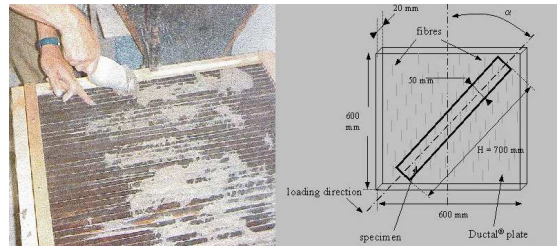


**Fig. 6:** Specific specimens with oriented fibres

Testing was performed in an MTS testing machine that features closed-loop servo control. The loading rate was held at 100 N/sec before the initial crack. The loading rate was then maintained at 0.01 mm/sec in order to ensure stable crack growth [Fig. 7].

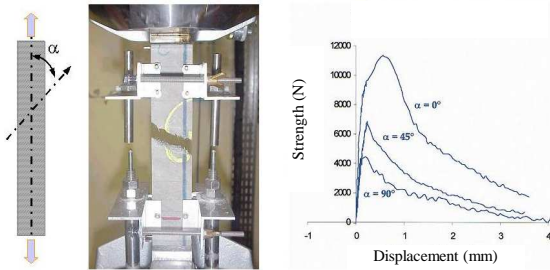
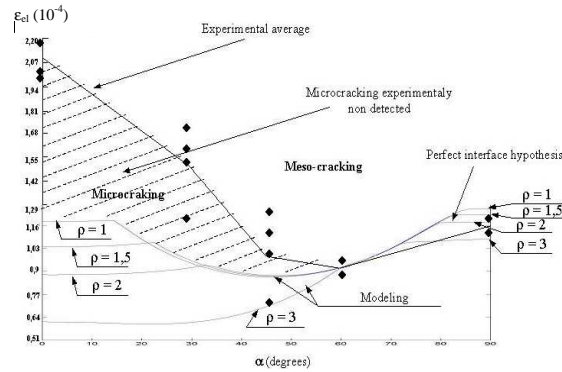


**Fig. 7:** Loading test conducted on specific specimens with oriented fibres

The first one occurs when the fibre direction lies in the loading direction ( $\alpha = 0^\circ$ ); the observed crack is then perpendicular to the tensile direction [Fig. 7]. According to the second situation, when  $\alpha$  is equal to  $45^\circ$ , the observed crack is in the loading direction, yet in most cases tends to propagate in the long fibre direction [Fig. 7]. Lastly, the third situation, when  $\alpha$  is equal to  $90^\circ$ , the observed crack is always perpendicular to the tensile direction [Fig. 7].

The maximum value of  $\epsilon_{el}$ , as obtained at the top of the linear part of the ascending branch of the load-displacement curve, has been identified when  $\alpha$  is equal to  $0^\circ$ . After this maximum value,  $\epsilon_{el}$  decreases with increasing  $\alpha$  over the range of  $0^\circ$ - $60^\circ$ . Once the minimum value has been reached,  $\epsilon_{el}$  increases with  $\alpha$  [Fig. 7]. This evolution of  $\epsilon_{el}$  with respect to angle  $\alpha$  would seem to lend support to our theoretical analysis based on a locally-anisotropic inclusion [Fig. 8].



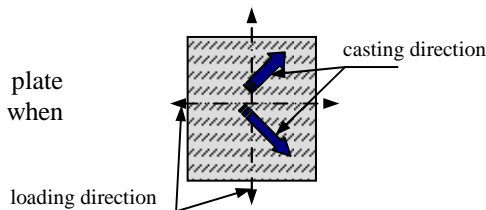
The various 1D damage laws governed by angle  $\alpha$  have been introduced into the model and then treated using the micro-plane method to yield a 3D phenomenological damage law for each cell, as governed by the angle  $\alpha$  between the primary tensile direction in the cell (given by the finite element method) and the fibre direction in the same cell.

**Fig. 8:** Comparison of experimental results with nucleation theory

#### 4. Modelling of an RPC structure

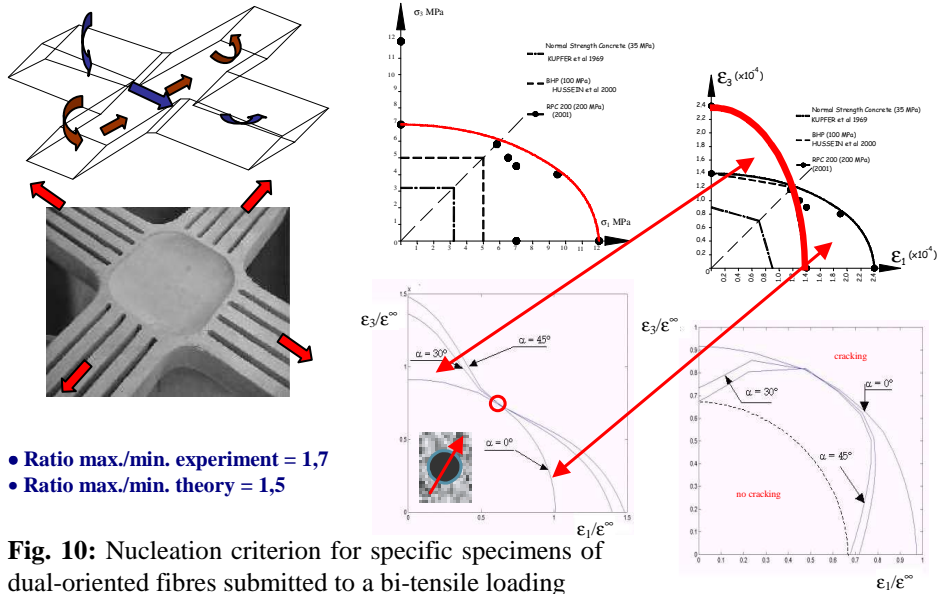
A structure is diagrammed by assembling cells of different densities and fibre orientations [ Fig. 3]. In order to take the interactions between cells into account in both the stress and strain distributions, we applied the finite element method. The localisation in each cell, which is analysed using the inclusion method, has also been affected by this interaction between cells in the same vicinity. In order to take this interaction into account, we adopted a simple method of superimposing the analytical localisation laws for adjacent cells [17]. According to this approach, we are able to reproduce the non-local effects governing the evolution of cracking [Fig. 4]. The localisation of damaged cells is also exposed to the damage tensor, so as to reproduce the decrease in the non-local reinforcing effect. As an illustration, we have studied a plate submitted to a proportional bi-tensile action. The best fibre orientation technique for casting this plate in RPC, in order to obtain the strongest plate under bi-tension, would be to orient the fibres [Fig. 9].

**Fig. 9:** Fibre distribution in the plate showing strongest behaviour when submitted to proportional bi-tension



## 5. Model improvements

This model was first tested in elasticity on the dual-oriented, fibre-reinforced RPC specimen of E. Astudillo [18]. The evolution in nucleation crack with angle  $\alpha$  depicts reality in a satisfactory manner [Fig. 10]. The problem then becomes how to find the best solution for modelling inside the structure.



The second test conducted on the model was intended to examine flexural and shear loadings of an RPC beam [Fig. 11]. The beam, with circular cutouts for the technical cables crossing the beam, is prestressed yet contains no passive reinforcement. The shear component is borne exclusively by the RPC. Two beams of this kind were cast and experimentally tested, with the fibre distributions in both beams being different. To proceed, we used a special comb in order to introduce a specific fibre direction into the beam.

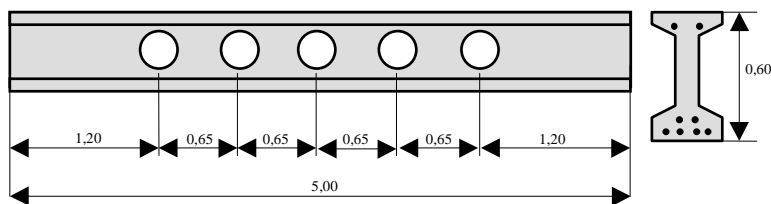


**Fig. 11:** Shape of the tested prestressed RPC beams



The first beam had been cast without use of this comb. The diagram of fibre distribution in the model [Fig. 12] calls for a horizontal fibre orientation in the upper, middle and lower parts of the structure.

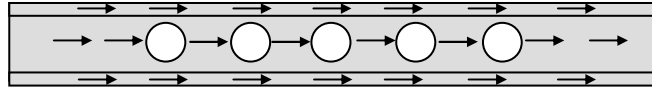


**Fig. 12:** Mode of casting and preferential fibre orientation in the first beam

The second beam was cast with a regular vertical penetration of the comb during casting so as to create vertical flow lines orienting the fibres within the middle part (central rib). The expectation behind such an action was to prevent the beam from developing horizontal cracks from one cutout to the next. The diagram of fibre distribution in the model [Fig. 13] shows a horizontal fibre orientation in the upper and lower hollow blocks, along with a vertical fibre orientation in the beam web.

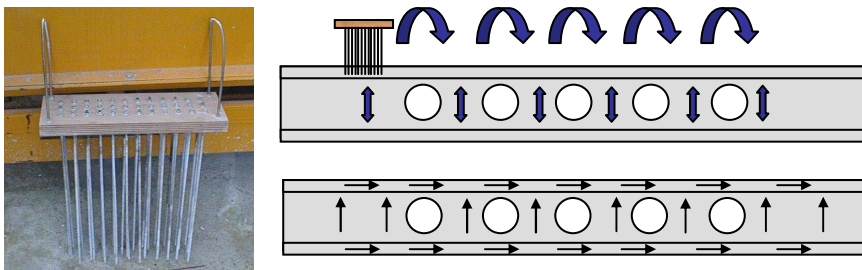


**Fig. 13:** Mode of casting and preferential fibre orientation in the second beam

No microcracks appeared in either of the two beams with just prestressing action; the flexural and shear loads were controlled by pressure applied using two jacks [Fig. 14].

The strength of the two beams in addition to the model results are given in Figure 15. The second beam proves to be 16% stronger than the first one cast, from the standpoint of the load-displacement curve [Fig. 15]. Model results confirm such observations and provide a good level of agreement with the stiffness model, given a certain height of microcracking.

Furthermore, the bond between RPC and prestressing cables has been reduced as the model always considers the bond to be perfect with perfect plasticity of the cable-modelling zones.

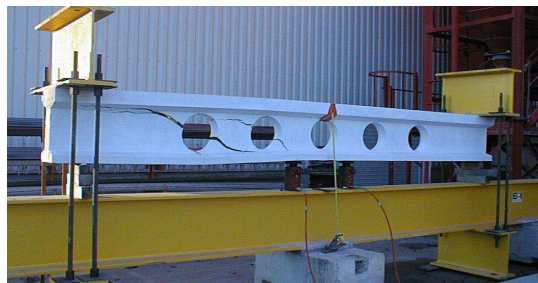


**Fig. 14:** Flexural and shear test on the RPC beams



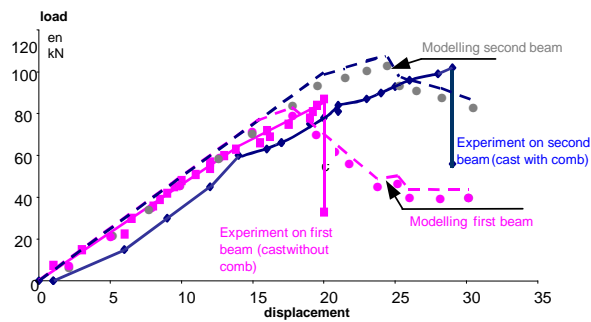


**Fig. 15:** Load-displacement curve of RPC beam behaviour

The numerical calculations are quite cumbersome using the "Matlab" software configuration for analytical calculus, in combination with the finite element approach. The internal heterogeneity approach was applied for a schematic representation of the entire structure. These steps lead to a three-scale analysis of a significant volume (beam length: 18 meters).

We could thereby reduce computational costs by conducting, as an initial step, a classical macroscopic elastic finite element analysis. This analysis would show the local loading of interest in studying the stress and strain fields with greater accuracy, by focusing on the present work in the area of internal heterogeneity.

## 6. Conclusion

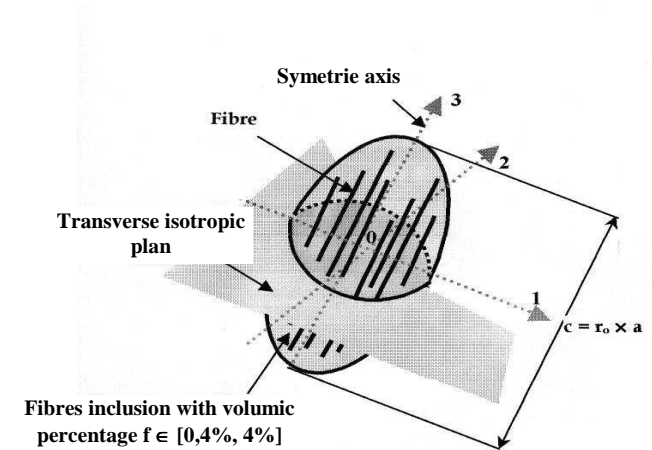
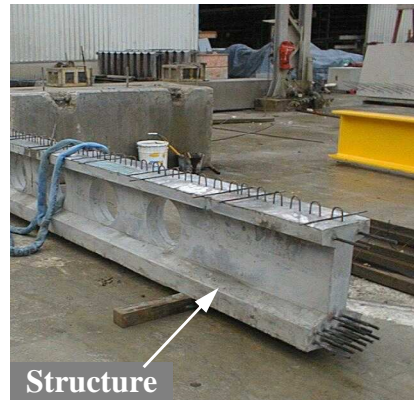
The analysis presented herein has focused on the nucleation and propagation of cracks on RPC specimens. A numerical study using both an analytical portion based on Eshelby's inclusion theory and superposition of localisation tensors has yielded a description of the microstructural stress and strain concentrations in any structure made of RPC for an arbitrary fibre distribution. A 3D model of crack propagation based on the micro-plane method has been obtained with 1D phenomenological laws extracted from tensile tests on specific specimens of unidirectional-oriented, fibre-reinforced RPC.

The improvement to experimental structural testing shows strong agreement between the nucleation determination model and microcrack development. The model successfully reproduces the influence of the local anisotropic distribution of fibres and its impact on the global behaviour of the structure. Such a tool could be used for evaluating the mechanical behaviour of a structure with a given fibre distribution. In this manner, the safety coefficient that takes casting variability into account could be determined for such a structure, while the best mode of casting could be approximated and best defined. In order to reduce computational costs, it would be advisable to conduct, as a first step, a classical macroscopic elastic finite element analysis in the defined structure submitted to a defined loading environment. This initial analysis will show the local loading where it would be beneficial to study stress and strain fields more accurately, by focusing on the present work in the area of internal heterogeneity. At this stage, the model can provide important information about the future mechanical behaviour of the structure.

## References

1. Cheyrezy, M., Maret, V., Frouin, L., Microstructural analysis of RPC. Cement and Concrete Research, Vol.25, n°7, pp.1491-1500 (1995)
2. Dugat, J., Roux, N., Bernier, G., Mechanical properties of RPC, Materials and Structures, Vol.29, pp.233-240 (1996)
3. Quemada, D., Rheology of Heterogeneous Fluids, Groupe Français de Rhéologie, 21<sup>ème</sup> Colloque annuel, Strasbourg, pp.1-13 (1986)
4. Bayard, O., Plé, O., An analysis of crack nucleation in fibre-reinforced concrete, 3, Werner and Fecht editors, Druckhaus Dresden publisher, pp. 718-721 (2000)
5. Plé, O., Bayard, O., Preliminary study of multiscale analysis in fibre reinforced concrete, Materials and Structures, Vol.35, June 2002, pp. 279-284
6. Bayard, O., Approche multi-échelles du comportement mécanique des BFUP, Thèse de Doctorat de l'Ecole Normale Supérieure de Cachan, (2003)
7. Eshelby, J., D., The force on an elastic singularity, Phil. Trans. Roy. Soc., A244, pp.87-112 (1951)
8. Eshelby, J., D., The elastic field outside an ellipsoidal inclusion, Proc. Roy. Soc., A252, pp. 561-569 (1959)
9. Bartos, P., Analysis of pull-out tests on fibres embedded in brittle matrices. J. Mat. Sci., Vol. 15, pp. 3122-3128, (1980)
10. Bartos, P., Review paper: bond in fibre reinforced cements and concretes. Int. J. Cem. Comp. Ltwt Concr., Vol. 3, pp. 159-177, (1981)
11. Gray, R., J., Analysis of the effect of embedded fibre length on fibre debonding and pull-out from an elastic matrix, Part 1: Review of theories. J. Mat. Sci., Vol. 19, pp. 861-870, (1984)
12. Greszczuk, L., B., Theoretical studies of the mechanics of the fibre-matrix interface in composites. In: ASTM STP 452. Philadelphia, pp. 42-58, (1969)
13. Kelly, A., Zweben, C., Poisson contraction in aligned fibre composites showing pull-out. J. Mat. Sci., pp. 582-587, (1976)
14. Pinchin, D., J., Tabor, D., Interfacial contact pressure and frictional stress transfer in steel fibre cement. RILEM Conference Testing and Test Methods of Fibre Cement Composites. UK: The Construction Press, pp. 337-344, (1978)
15. Cook, J., Gordon, J., E., A mechanism for the control of crack propagation in all brittle systems. Proc. Roy. Soc., 282A, pp.508-520, (1964)
16. Majumdar, A., J., Properties of fibre reinforced composites. Fibre Reinforced Cement and Concrete, RILEM, UK: The construction Press, pp. 279-313, (1975)
17. Plé, O., Bayard, O., Preliminary modelisation of internal heterogeneities in fibre reinforced concrete, Materials and Structures, RILEM Publications, under submission
18. Astudillo de la Vega, E., Etude expérimentale du comportement mécanique d'un BFUP en traction bi-axiale, Thèse de Doctorat de l'ENS Cachan et de l'Université Paris VI (2002)





Shape of the structure

Parameterized cluster in each cell

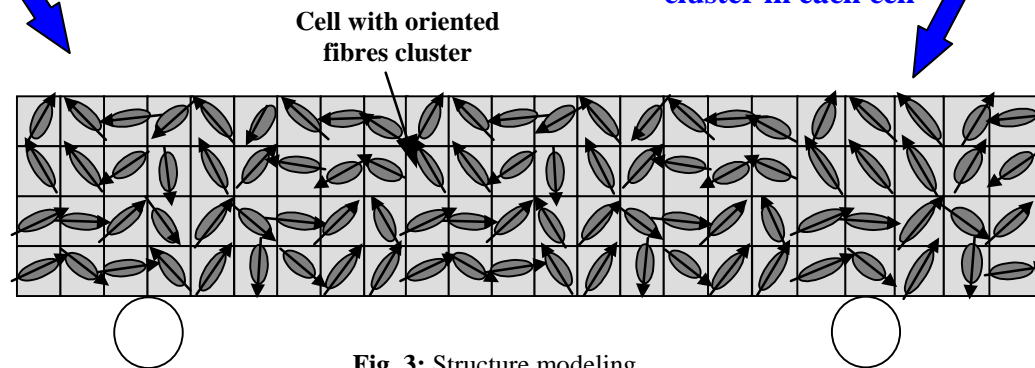


Fig. 3: Structure modeling